Supplement of Biogeosciences, 23, 5607–5624, 2026
https://doi.org/10.5194/bg-23-5607-2026-supplement

Biogeosciences Open Access EGU

Supplement of

AngleCam V2: Predicting leaf inclination angles across taxa from daytime and nighttime photos

Luis Kremer et al.

Correspondence to: Luis Kremer (luis.kremer@geosense.uni-freiburg.de)

S1 Genus representation across datasets

Table S1: Genus-level representation across training, validation, and phylogenetic analysis (PA) datasets. Training and validation counts show the number of images per genus used for model development. Phylogenetic analysis includes three samples per genus where available, with mean absolute error (MAE) values representing the mean absolute deviation between AngleCam V2 predictions and labeled leaf inclination angle distribution references in degrees. Empty MAE values (—) indicate genera not included in the phylogenetic analysis. Genera are ordered by phylogenetic data availability and total sample count.

Genus	Training	Validation	Total	PA	MAE (°)
Tilia	1014	249	1263	3	3.92
Acer	714	179	893	3	3.94
Quercus	198	60	258	3	10.61
Fagus	191	35	226	3	7.99
Carpinus	119	29	148	3	12.75
Fraxinus	107	31	138	3	10.62
Sorbus	93	31	124	3	7.76
Eucalyptus	86	20	106	3	3.32
Rhododendron	86	17	103	3	7.29
Aesculus	76	23	99	3	11.67
Mespilus	40	14	54	3	9.70
Betula	41	11	52	3	7.63
Salix	30	10	40	3	6.24
Cynophalla	28	8	36	3	6.98
Prunus	24	11	35	3	11.07
Cornus	26	7	33	3	9.71
Sasa	24	6	30	3	4.94
Syringa	25	5	30	3	10.73
Crinum	25	1	26	3	7.40
Magnolia	19	7	26	3	4.23
Ocimum	22	4	26	3	2.71
Alnus	18	6	24	3	5.61
Rhytidophyllum	18	6	24	3	8.41
Olea	18	5	23	3	14.72
Pachystachys	17	6	23	3	3.00
Arbutus	17	5	22	3	14.48
Bixa	17	4	21	3	9.54
Cercis	15	4	19	3	7.46
Styrax	14	4	18	3	5.51
Deherainia	14	2	16	3	7.49
Hedera	11	4	15	3	2.75
Pyrus	13	2	15	3	5.91
Dracaena	13	1	14	3	6.02
Xylopia	11	3	14	3	10.79
Berberis	12	1	13	3	8.16
Coleus	10	3	13	3	6.47
Corylus	7	5	12	3	8.94
Laurus	8	4	12	3	10.40

Continued on next page

Table S1 – continued from previous page

Genus	Training	Validation	Total	PA	MAE (°)
Pilea	10	2	12	3	1.14
Ulmus	10	2	12	3	8.53
Alliaria	10	1	11	3	4.72
Clematis	10	1	11	3	11.24
Crassula	10	1	11	3	6.03
Ctenanthe	7	4	11	3	10.85
Euphorbia	11	0	11	3	5.82
Lavandula	9	2	11	3	13.99
Oplismenus	11	0	11	3	3.96
Rubus	8	3	11	3	4.37
Buxus	8	1	9	3	11.96
Goudaea	7	2	9	3	1.43
Passiflora	8	1	9	3	6.46
Epipremnum	8	0	8	3	8.38
Ficus	5	3	8	3	4.78
Heliconia	6	2	8	3	4.36
Hypericum	7	0	7	3	2.48
Urceolina	5	2	7	3	10.58
Viburnum	6	1	7	3	10.51
Adiantum	5	1	6	3	9.16
Begonia	5	1	6	3	3.98
Brachychiton	6	0	6	3	5.22
Callianthe	5	1	6	3	4.83
Diospyros	6	0	6	3	1.67
Ilex	5	1	6	3	5.14
Ligustrum	5	1	6	3	8.79
Platanus	4	2	6	3	7.74
Sambucus	6	0	6	3	10.88
Acacia	4	1	5	3	9.22
Asplenium	4	1	5	3	11.03
Carex	2	3	5	3	1.73
Eupomatia	4	1	5	3	3.16
Simmondsia	3	2	5	3	13.25
Fittonia	4	0	4	3	4.32
Hippophae	2	2	4	3	8.07
Malus	4	0	4	3	7.25
Microcitrus	4	0	4	3	7.65
Tripsacum	3	1	4	3	4.81
Zantedeschia	4	0	4	3	3.19
Corymbia	2	1	3	3	4.47
Eugenia	1	2	3	3	7.49
Melicytus	3	0	3	3	6.83
Rhus	1	2	3	3	3.78
Robinia	3	0	3	3	3.82
Tetradium	3	0	3	3	2.52
Arctostaphylos	2	0	2	3	7.82
Carpenteria	2	0	2	3	7.39
Ceratonia	2	0	2	3	8.75

Continued on next page

Table S1 – continued from previous page

Genus	Training	Validation	Total	PA	MAE (°)
Correa	2	0	2	3	11.48
Juglans	2	0	2	3	5.36
Lyonothamnus	2	0	2	3	3.69
Philadelphus	2	0	2	3	6.85
Solanum	1	1	2	3	11.06
Beaucarnea	1	0	1	3	10.84
Cotoneaster	1	0	1	3	10.73
Dactylis	1	0	1	3	5.02
Deutzia	1	0	1	3	10.57
Diplacus	0	1	1	3	6.17
Lonicera	1	0	1	3	9.53
Nothofagus	1	0	1	3	1.44
Spiraea	1	0	1	3	3.21
Tradescantia	1	0	1	3	1.51
Goeppertia	19	1	20	—	—
Maranta	9	3	12	—	—
Aglaonema	2	1	3	—	—
Chimonobambusa	3	0	3	—	—
Erica	2	1	3	—	—
Kumara	1	2	3	—	—
Lasiopetalum	3	0	3	—	—
Liriodendron	1	2	3	—	—
Morus	3	0	3	—	—
Reynoutria	2	1	3	—	—
Skimmia	3	0	3	—	—
Xiphidium	3	0	3	—	—
Buddleja	2	0	2	—	—
Castanea	1	1	2	—	—
Hosta	1	1	2	—	—
Miconia	2	0	2	—	—
Ostrya	2	0	2	—	—
Paliurus	1	1	2	—	—
Sedum	2	0	2	—	—
Selaginella	2	0	2	—	—
Spathiphyllum	2	0	2	—	—
Zelkova	1	1	2	—	—
Aria	1	0	1	—	—
Crataegus	1	0	1	—	—
Dimorphotheca	1	0	1	—	—
Doryanthes	1	0	1	—	—
Gustavia	1	0	1	—	—
Spyridium	0	1	1	—	—
Vaccinium	1	0	1	—	—

S2 Pseudo-NIR generation examples

Visual examples of the pseudo-NIR pipeline are compared to actual night-vision NIR imagery across ten forest scenes (Fig. S1). These scenes represent two tree species: European beech

(*Fagus sylvatica* L.) and European hornbeam (*Carpinus betulus* L.). Images were acquired in 2025 at the ECOSENSE site (Ettenheim, Germany) and the Hartheim Forest Research Site (Germany). The selection covers diverse canopy conditions, including clear skies (Fig. S1, rows 2, 3, 5, 6, 7), direct solar radiation (row 3), pronounced daytime shadows (rows 5, 6, 7), and rain (row 1). Phenological stages range from leaf onset (row 4) to leaf senescence (rows 2, 10).

The ten selected scenes show a good agreement in illumination falloff between the generated pseudo-NIR images (Fig. S1, column d) and the actual NIR imagery (Fig. S1, column e). Although grayscale images (column b) reduce the model's dependence on color-specific features, they do not necessarily reflect the night-vision environment. Columns (d) and (e) consistently show patterns in which foreground vegetation is highlighted by increased brightness, while distant backgrounds fade into darkness. This effect reduces background detail to levels characteristic of NIR imagery, whereas grayscale scenes (column b) often preserve unrealistic detail at greater distances. Additionally, the pseudo-NIR approach eliminates "blue sky" effects by darkening the background (Fig. S1, rows 2, 5), thereby aligning with the monochromatic response of night-vision sensors.

Despite its potential as a training proxy, the pseudo-NIR pipeline has several inherent limitations. Actual NIR images show high vegetation reflectance, making leaves appear bright and uniform. While the pseudo-NIR pipeline replicates this effect, leaves located very close to the camera become excessively bright, leading to localized overexposure. Since grayscale and ultimately pseudo-NIR images are derived from daytime RGB photos, they retain ambient shadows determined by the sun's position. In contrast, actual NIR imagery captured with NIR-LEDs typically exhibits minimal shadowing on surfaces directly facing the camera. This discrepancy becomes strongly evident under lens flare conditions (Fig. S1, row 3), where the pseudo-NIR image contains overexposure and light stripes that are absent in real night-vision scenes. Furthermore, the illumination falloff with increasing distance is often more pronounced in the pseudo-NIR pipeline than in actual NIR imagery. In certain cases, actual NIR imagery preserves more background detail than its synthetic counterpart (Fig. S1, rows 3, 7, 10). This difference is most pronounced in the deep background and less pronounced in images focused on vegetation near the camera (Fig. S1, rows 1, 5, 6, 9).

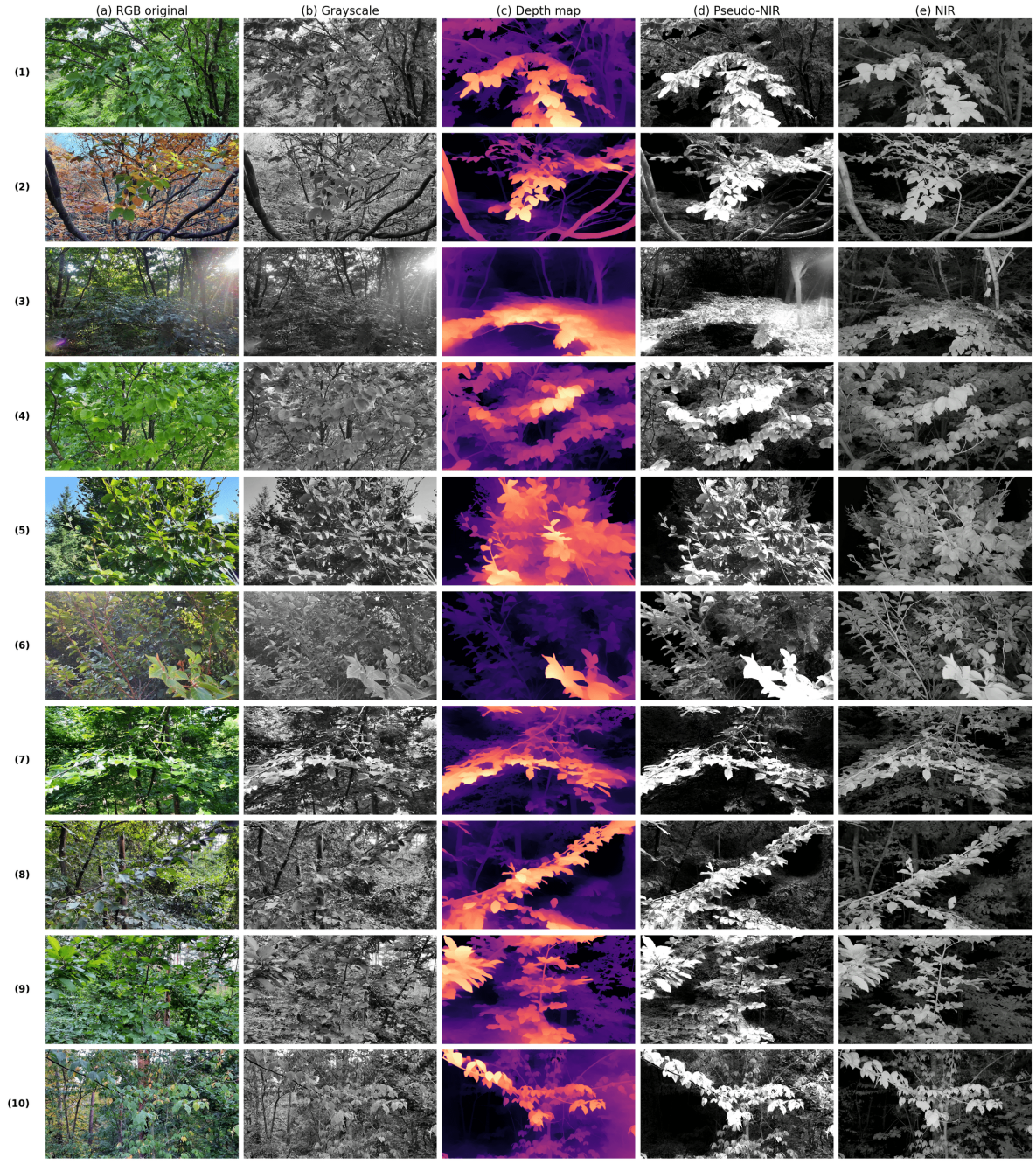

Figure S1: Visual examples of the pseudo-NIR image generation pipeline across ten different forest scenes (1–10). The columns represent the sequential transformation steps: (a) the original RGB photograph, (b) conversion to grayscale, (c) per-pixel depth estimation using Depth Anything V2, (d) the generated pseudo-NIR image simulating distance-based illumination falloff, and (e) the actual NIR night-vision image of the same scene captured during the nighttime period for reference.